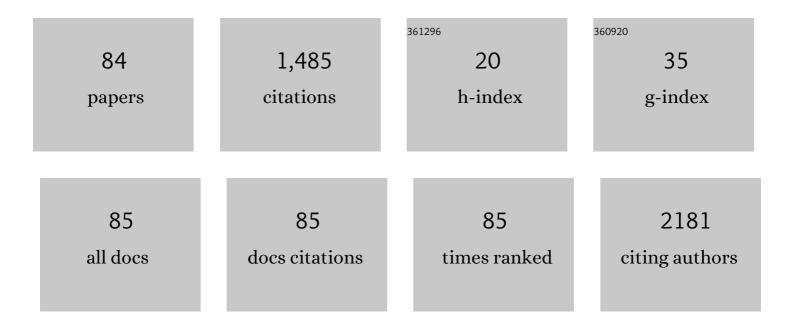
List of Publications by Year in descending order

Source: https://exaly.com/author-pdf/1592618/publications.pdf Version: 2024-02-01



LOUISA MESHI

#	Article	IF	CITATIONS
1	Assembly of mesoscale helices with near-unity enantiomeric excess and light-matter interactions for chiral semiconductors. Science Advances, 2017, 3, e1601159.	4.7	135
2	New Nanocrystalline Materials: A Previously Unknown Simple Cubic Phase in the SnS Binary System. Nano Letters, 2015, 15, 2174-2179.	4.5	126
3	Self-Assembly and Structure of Directly Imaged Inorganic-Anion Monolayers on a Gold Nanoparticle. Journal of the American Chemical Society, 2009, 131, 17412-17422.	6.6	102
4	Heat treatments' effects on the microstructure and mechanical properties of an equiatomic Al-Cr-Fe-Mn-Ni high entropy alloy. Materials Science & Engineering A: Structural Materials: Properties, Microstructure and Processing, 2017, 689, 384-394.	2.6	71
5	Long-period antiphase domains and short-range order in a B2 matrix of the AlCoCrFeNi high-entropy alloy. Scripta Materialia, 2017, 139, 49-52.	2.6	65
6	Defect reduction in GaN/(0001)sapphire films grown by molecular beam epitaxy using nanocolumn intermediate layers. Applied Physics Letters, 2008, 92, .	1.5	63
7	Addressing the issue of precipitates in maraging steels – Unambiguous answer. Materials Science & Engineering A: Structural Materials: Properties, Microstructure and Processing, 2015, 638, 232-239.	2.6	63
8	Electrochemical Intercalation of Lithium Ions into NbSe ₂ Nanosheets. ACS Applied Materials & Interfaces, 2016, 8, 11390-11395.	4.0	56
9	Direct Imaging of the Ligand Monolayer on an Anion-Protected Metal Nanoparticle through Cryogenic Trapping of its Solution-State Structure. Journal of the American Chemical Society, 2008, 130, 16480-16481.	6.6	45
10	The relation between Mn additions, microstructure and corrosion behavior of new wrought Mg-5Al alloys. Materials Characterization, 2018, 145, 101-115.	1.9	42
11	Dislocation structure and hardness of surface layers under friction of copper in different lubricant conditions. Acta Materialia, 2011, 59, 342-348.	3.8	38
12	Friction stir welded AM50 and AZ31 Mg alloys: Microstructural evolution and improved corrosion resistance. Materials Characterization, 2017, 126, 86-95.	1.9	33
13	Retardation of the Ï f phase formation in the AlCoCrFeNi multi-component alloy. Materials Characterization, 2019, 148, 171-177.	1.9	28
14	Nanometric diamond delta doping with boron. Physica Status Solidi - Rapid Research Letters, 2017, 11, 1600329.	1.2	27
15	Deformation in nanocrystalline ceramics: A microstructural study of MgAl2O4. Acta Materialia, 2020, 183, 137-144.	3.8	27
16	Defect-controlled growth of GaN nanorods on (0001)sapphire by molecular beam epitaxy. Applied Physics Letters, 2008, 93, 111911.	1.5	24
17	Friction, wear and structure of Cu samples in the lubricated steady friction state. Tribology International, 2012, 46, 154-160.	3.0	22
18	Identification of the structure of a new Al–U–Fe phase by electron microdiffraction technique. Journal of Alloys and Compounds, 2002, 347, 178-183.	2.8	21

#	Article	IF	CITATIONS
19	Effect of oxygen pressure on structure and ionic conductivity of epitaxial Li _{0.33} La _{0.55} TiO ₃ solid electrolyte thin films produced by pulsed laser deposition. RSC Advances, 2016, 6, 61974-61983.	1.7	21
20	Orientations of polyoxometalate anions on gold nanoparticles. Dalton Transactions, 2012, 41, 9849.	1.6	20
21	Determination of the structure of UFe2Al10 compound. Journal of Alloys and Compounds, 2004, 370, 206-210.	2.8	19
22	Thermodynamic modeling of Al–U–X (X = Si,Zr). Journal of Nuclear Materials, 2015, 464, 170-184.	1.3	19
23	Characterization of new aluminides found in the ThT2Al20 alloys (where T = Ti, V, Mn). Journal of Alloys and Compounds, 2015, 641, 1-6.	2.8	19
24	Understanding the Role of the Constituting Elements of the AlCoCrFeNi High Entropy Alloy through the Investigation of Quaternary Alloys. Metals, 2020, 10, 1275.	1.0	19
25	Elastic consideration of the precipitation in model alloys of maraging steels: theory and experimental validation. Journal of Materials Science, 2015, 50, 4970-4979.	1.7	18
26	Size-dependent spin state and ferromagnetism in La0.8Ca0.2CoO3 nanoparticles. Journal of Applied Physics, 2010, 108, 063907.	1.1	17
27	Regioselective placement of alkanethiolate domains on tetrahedral and octahedral gold nanocrystals. Chemical Communications, 2012, 48, 9765.	2.2	14
28	Abrupt symmetry decrease in the ThT2Al20 alloys (TÂ=Â3d transition metal). Journal of Alloys and Compounds, 2015, 648, 353-359.	2.8	14
29	Increased corrosion resistance of the AZ80 magnesium alloy by rapid solidification. Journal of Biomedical Materials Research - Part B Applied Biomaterials, 2015, 103, 1541-1548.	1.6	14
30	The structure of the ternary aluminide ThFe2Al10. Intermetallics, 2005, 13, 792-795.	1.8	13
31	A study of the Al-rich part of the Al–Ni–Pt alloy system. Journal of Alloys and Compounds, 2012, 514, 60-63.	2.8	13
32	Atomic structure solution of the complex quasicrystal approximant Al ₇₇ Rh ₁₅ Ru ₈ from electron diffraction data. Acta Crystallographica Section B: Structural Science, Crystal Engineering and Materials, 2014, 70, 999-1005.	0.5	13
33	Shock wave characterization of precipitate strengthening of PH 13–8 Mo stainless steel. Acta Materialia, 2020, 187, 176-185.	3.8	13
34	Polyoxometalate-directed assembly of water-soluble AgCl nanocubes. Chemical Communications, 2012, 48, 2207.	2.2	12
35	New complex intermetallic in the Al–Rh–Ru alloy system. Journal of Alloys and Compounds, 2011, 509, 6551-6555.	2.8	11
36	Why UFexAl12â^'x phase does not crystallize with ThMn12-structure type, when xÂ=Â2?. Intermetallics, 2011, 19, 713-720.	1.8	11

#	Article	IF	CITATIONS
37	New ordered phase in the quasi-binary UAl ₃ –USi ₃ system. Acta Crystallographica Section B: Structural Science, Crystal Engineering and Materials, 2014, 70, 580-585.	0.5	11
38	Novel AlCrFeNiNb0.3 high entropy alloy: Microstructure, properties and an unknown Nb-rich intermetallide. Intermetallics, 2020, 127, 106965.	1.8	10
39	Tetragonal phase in Al-rich region of U–Fe–Al system. Journal of Alloys and Compounds, 2005, 402, 84-88.	2.8	9
40	Combinatorial synthesis and high-throughput characterization of the thin film materials system Co-Mn-Ge: Composition, structure, and magnetic properties. Physica Status Solidi (A) Applications and Materials Science, 2015, 212, 1969-1974.	0.8	9
41	In-depth characterization of stacking faults forming during the growth of Transition-Metal Di-Chalcogenides (TMDCs) by ambient pressure-CVD. Materials Characterization, 2022, 184, 111666.	1.9	9
42	The reduction of threading dislocations in GaN using a GaN nanocolumn interlayer. Physica Status Solidi C: Current Topics in Solid State Physics, 2008, 5, 1645-1647.	0.8	8
43	An investigation of the Al–Rh–Ru phase diagram above 50at.% Al. Journal of Alloys and Compounds, 2011, 509, 8018-8021.	2.8	8
44	Microstructural Evolution of Cr-Rich ODS Steels as a Function of Heat Treatment at 475°C. Metallography, Microstructure, and Analysis, 2012, 1, 158-164.	0.5	8
45	Sensitivity of thermo-electric power measurements to α‑ʿα′ phase separation in Cr-rich oxide dispersion strengthened steels. Journal of Materials Science, 2015, 50, 4629-4635.	1.7	8
46	Shock wave determination of temperature dependence of twinning stress in vanadium and tantalum. Materials Science & Engineering A: Structural Materials: Properties, Microstructure and Processing, 2022, 833, 142537.	2.6	8
47	A study of the Al–Pd–Pt alloy system. Journal of Alloys and Compounds, 2014, 600, 125-129.	2.8	7
48	Formation of Complex Intermetallics in the Al-Rich Part of Al-Pt-Ru. Journal of Phase Equilibria and Diffusion, 2015, 36, 327-332.	0.5	7
49	Ordered U(Al, Si)3 phase: Structure and bonding. Journal of Alloys and Compounds, 2017, 690, 884-889.	2.8	7
50	GaN devices based on nanorods. Journal of Physics: Conference Series, 2010, 209, 012001.	0.3	6
51	Strategies for full structure solution of intermetallic compounds using precession electron diffraction zonal data. Journal of Applied Crystallography, 2014, 47, 1032-1041.	1.9	6
52	A study of the Al–Pt–Ir phase diagram. Journal of Alloys and Compounds, 2015, 646, 873-878.	2.8	6
53	Crystal structures of the Al–Ti–Pt τ5 and τ6 phases solved by zonal precession electron diffraction. Journal of Alloys and Compounds, 2015, 621, 47-52.	2.8	6
54	Crystal structure of the Th 2 Ni 10 Al 15 phase solved using electron diffraction tomography. Journal of Alloys and Compounds, 2016, 660, 496-502.	2.8	6

#	Article	IF	CITATIONS
55	Characterization of Atomic Structures of Nanosized Intermetallic Compounds Using Electron Diffraction Methods. Advanced Materials, 2018, 30, e1706704.	11.1	6
56	Radiation Resistance of the U(Al, Si)3 Alloy: Ion-Induced Disordering. Materials, 2018, 11, 228.	1.3	6
57	Characterization of nano-sized particles in 14%Cr oxide dispersion strengthened (ODS) steel using classical and frontier microscopy methods. Materials Characterization, 2020, 160, 110075.	1.9	6
58	Identification of a new hexagonal phase in the Al–Cu–Re system. Journal of Alloys and Compounds, 2009, 488, 108-111.	2.8	5
59	New orthorhombic phase in U–Fe–Al–Si system. Journal of Alloys and Compounds, 2011, 509, 206-209.	2.8	5
60	Structure and peculiarities of bonding in the Al-rich A-Mn-Al alloys (where A=Y, Gd, Th and U). Intermetallics, 2018, 100, 44-51.	1.8	5
61	Electroplating of Pure Aluminum from [HMIm][TFSI]–AlCl3 Room-Temperature Ionic Liquid. Coatings, 2021, 11, 1414.	1.2	5
62	Determination of the structure of a new tetragonal U2FeAl20 phase. Journal of Alloys and Compounds, 2008, 460, 196-200.	2.8	4
63	Crystal structure of a new quaternary Mg–Zn–Ca–Li phase. Intermetallics, 2012, 22, 62-67.	1.8	4
64	Refinement of the Al-rich part of the Al–Cu–Re phase diagram and atomic model of the ternary Al6.2Cu2Re phase. Journal of Alloys and Compounds, 2016, 670, 18-24.	2.8	4
65	Influence of alloying elements and the state of order on the formation of antiphase boundaries in B2 phases. Intermetallics, 2022, 141, 107434.	1.8	4
66	Crystal structure of the Al2CuIr phase. Journal of Alloys and Compounds, 2010, 496, 208-211.	2.8	3
67	Bonding and Stability of Ternary Structures in the CeT2Al20 (T=Ta, W, Re) and YRe2Al20 Alloys. Metals, 2020, 10, 422.	1.0	3
68	Structural study of Al78Mn17.5Pt4.5 and (re)constitution of the Al–Mn–Pt system in its vicinity. Journal of Alloys and Compounds, 2021, 861, 158328.	2.8	3
69	Liquidus projection of Al-rich corner of the ternary Al–Fe–U system. Intermetallics, 2010, 18, 2119-2123.	1.8	2
70	Study of ternary complex Al—Mg—Ag intermetallides using Precession Electron Diffraction. Zeitschrift Fur Kristallographie - Crystalline Materials, 2013, 228, 59-62.	0.4	2
71	The origin of the effect of aging on the thermoelectric power of maraging C250 steel. Journal of Materials Science, 2015, 50, 7698-7704.	1.7	2
72	Explanation of structural differences and similarities between the AT ₂ Al ₁₀ phases (where A=actinide, lanthanide or rare earth element and T=transition metal). Zeitschrift Fur Kristallographie - Crystalline Materials, 2019, 234, 595-603.	0.4	2

LOUISA MESHI

#	Article	IF	CITATIONS
73	Structure characterization of novel alluminides in the Nd-Re-Al system by electron crystallography methods. Materials Characterization, 2020, 168, 110562.	1.9	2
74	Addressing a "Black Box―of Bottom-Up Synthesis: Revealing the Structures of Growing Colloidal-Nanocrystal Nuclei. Inorganic Chemistry, 2015, 54, 10521-10523.	1.9	1
75	Shock-induced twinning in polycrystalline vanadium: II. Surface layer. Materials Characterization, 2021, 175, 111062.	1.9	1
76	Nano-pendeo GaN Growth of Light Emitting Devices on Silicon. Journal of Light and Visual Environment, 2008, 32, 187-190.	0.2	1
77	Electron Diffraction Study of the Space Group Variation in the Al–Mn–Pt T-Phase. Symmetry, 2022, 14, 38.	1.1	1
78	Direct observation of initial stages of precipitation hardening process in commercial Al 6061 alloy. Journal of Materials Science, 2022, 57, 10395-10406.	1.7	1
79	Characterization of structural defects in highly mismatched GaP nanowires. Materials Letters, 2013, 113, 38-41.	1.3	0
80	Evaluation of microstructural damage and alteration of polytypes to determine the aging of silicon carbide. , 2013, , .		0
81	Kinetics of the α-α′ phase separation in a 14%Cr oxide dispersion steel at intermediate temperatures. Materials Letters, 2021, 285, 129088.	1.3	0
82	Structural changes as a function of transition metal's (T) type in the ThT2Al20 alloys. Acta Crystallographica Section A: Foundations and Advances, 2016, 72, s236-s236.	0.0	0
83	Structure of <i>A</i> – <i>T</i> –Al aluminides (<i>A</i> = actinide/lanthanide; <i>T</i> = transition) Tj ETQq2	l 1.0,7843	314,rgBT /O∨
84	Structure solution of the Al _{69.2} Cu ₂₀ Cr _{10.8} ï• phase. Journal of Applied Crystallography, 2022, 55, 74-79.	1.9	0